The soil water characteristic as new class of closed-form parametric expressions for the flow duration curve

Mojtaba Sadegh,[1] Jasper A. Vrugt,[1,2], and Hoshin V. Gupta,[3]

Corresponding author: Jasper A. Vrugt, Department of Civil and Environmental Engineering, University of California, Irvine, USA. (jasper@uci.edu)

[1]Department of Civil and Environmental Engineering, University of California, Irvine, USA.

[2]Department of Earth System Science, University of California, Irvine, CA, USA.

[3]Department of Hydrology and Water Resources, University of Arizona, Tucson, CA, USA.

Abstract. The flow duration curve is a signature catchment characteristic that depicts graphically the relationship between the exceedance probability of streamflow and its magnitude. This curve is relatively easy to create and interpret, and is used widely for hydrologic analysis, water quality management, and the design of hydroelectric power plants (among others). Several mathematical formulations have been proposed to mimic the FDC. Yet, these efforts have not been particularly successful, in large part because available functions are not flexible enough to portray accurately the functional shape of the FDC for a large range of catchments and contrasting hydrologic behaviors. Here, we extend the work of *Vrugt and Sadegh* [2013] and introduce several commonly used models of the soil water characteristic as new class of closed-form parametric expressions for the flow duration curve. These soil water retention functions are relatively simple to use, contain between two to five parameters, and mimic closely the empirical FDCs of 408 catchments of the MOPEX data set. If quality of fit is of main importance then the 5-parameter bimodal retention function of Kosugi is preferred, whereas a 2-parameter formulation of this model is deemed superior for diagnostic analysis as the fitting coefficients are well defined and exhibit a negligible correlation.

1. Introduction

The flow duration curve (FDC) is a widely used characteristic signature of a watershed, and is one of the three most commonly used graphical methods in hydrologic studies, along with the mass curve and the hydrograph [*Foster*, 1934]. The FDC relates the exceedance probability (frequency) of streamflow to its magnitude, and characterizes both the flow regime and the streamflow variability of a watershed. It is closely related to "survival" function in statistics [*Vogel and Fennessey*, 1994], and is interpreted as a complement to the streamflow cumulative distribution function (CDF). The FDC is frequently used to predict the distribution of streamflow for water resources planning purposes, to simplify analysis of water resources problems, and to communicate watershed behavior to those who lack in-depth hydrologic knowledge. One should be particularly careful to rely solely on the FDC as main descriptor of catchment behavior [*Vogel and Fennessey*, 1995] as the curve represents the rainfall-runoff as disaggregated in the time domain and hence lacks temporal structure [*Searcy*, 1959; *Vogel and Fennessey*, 1994].

The first application of the FDC dates back to 1880 and appears in the work by Clemens Herschel [*Foster*, 1934]. Ever since, the FDC has been used in many fields of study including (among others) the design and operation of hydropower plants [*Singh et al.*, 2001], flow diversion and irrigation planning [*Chow*, 1964; *Warnick*, 1984; *Pitman*, 1993; *Mallory and McKenzie*, 1993], streamflow assessment and prediction [*Tharme*, 2003], sedimentation [*Vogel and Fennessey*, 1995], water quality management [*Mitchell*, 1957; *Searcy*, 1959; *Jehng-Jung and Bau*, 1996], waste-water treatment design [*Male and Ogawa*, 1984], and low-flow analysis [*Wilby et al.*, 1994; *Smakhtin*, 2001; *Pfannerstill et al.*, 2014].

Recent studies have used the FDC as a benchmark for quality control [*Cole et al.*, 2003], and signature or metric for model calibration and evaluation [*Refsgaard and Knudsen*, 1996; *Yu and Yang*, 2000; *Wagener and Wheater*, 2006; *Son and Sivapalan*, 2007; *Yadav et al.*, 2007; *Yilmaz et al.*, 2008; *Zhang et al.*, 2008; *Blazkova and Beven*, 2009; *Westerberg et al.*, 2011; *Vrugt and Sadegh*, 2013; *Pfannerstill et al.*, 2014; *Sadegh and Vrugt*, 2014a; *Sadegh et al.*, 2014b]. For instance, *Vrugt and Sadegh* [2013] used the fitting coefficients of a simple parametric expression of the FDC as summary statistics in diagnostic model evaluation with approximate Bayesian computation (ABC).

Application of FDCs for hypothesis testing [*Kavetski et al.*, 2011] can improve identifiability and help attenuate the problems associated with traditional residual-based objective (likelihood) functions (e.g. Nash-Sutcliffe, sum of squared residuals, absolute error, relative error) that emphasize fitting specific parts of the hydrograph, such as high or low flows [*Schaefli and Gupta*, 2007; *Kavetski et al.*, 2011; *Westerberg et al.*, 2011], and thereby lose important information regarding the structural inadequacies of the model [*Gupta et al.*, 2008, 2012; *Vrugt and Sadegh*, 2013]. The FDC is a signature watershed characteristic that along with other hydrologic metrics, can help shed lights on epistemic (model structural) errors [*Euser et al.*, 2013; *Vrugt and Sadegh*, 2013]. For example, *Son and Sivapalan* [2007] used the FDC to highlight the reasons of model malfunctioning and to propose improvements to the structure of their conceptual water balance model for the watershed under investigation. Indeed, a deep groundwater flux was required to simulate adequately dominant low flows of the hydrograph. *Yilmaz et al.* [2008] in a similar effort to improve simulation of the vertical distribution of soil moisture in the HL-DHM model, used the slope of the FDC as benchmark for model performance. The FDC was deemed

suitable for this purpose due to its strong dependence on the simulated soil moisture distribution, and relative lack of sensitivity to rainfall data and timing errors. However, the proposed refinements of the HL-DHM model were found inadequate and this failure was attributed to the inherent weaknesses of the conceptual structure of HL-DHM.

The usefulness of duration curves (e.g. precipitation [*Yokoo and Sivapalan*, 2011], baseflow [*Kunkle*, 1962] and streamflow (flow) [*Hughes and Smakhtin*, 1996]) depends in large part on the temporal resolution of the data (e.g. quarterly, hourly, daily, weekly, and monthly) these curves are constructed from. FDCs derived from daily streamflow data are commonly considered to warrant an adequate analysis of the hydrologic response of a watershed [*Vogel and Fennessey*, 1994; *Smakhtin*, 2001; *Wagener and Wheater*, 2006; *Zhao et al.*, 2012]. For example, a FDC with a steep mid section (also referred to as slope) is characteristic for a watershed that responds quickly to rainfall, and thus has a small storage capacity and large ratio of direct runoff to baseflow. A more moderate slope, on the contrary, is indicative of a basin whose streamflow response reacts much slower to precipitation forcing with discharge that is made up in large part of baseflow [*Yilmaz et al.*, 2008].

The shape of the FDC is determined by several factors including (amongst others) topography, physiography, climate, vegetation cover, land use, and storage capacity [*Singh*, 1971; *Lane et al.*, 2005; *Zhao et al.*, 2012], and can be used to perform regional analysis [*Wagener and Wheater*, 2006; *Masih et al.*, 2010] or to cluster catchments into relatively homogeneous groups that exhibit a relatively similar hydrologic behavior [*Coopersmith et al.*, 2012; *Sawicz et al.*, 2011]. Different studies have appeared in the hydrologic literature that have analyzed how the shape of the FDC is affected by physiographic factors

and/or vegetation cover. Despite this progress made, interpretation of the FDC can be controversial if an insufficiently long streamflow data record is used [*Vogel and Fennessey*, 1994]. The lower end of the FDC (low flows) is particularly sensitive to the period of study, and to whether the streamflow data includes severe droughts or not [*Castellarin et al.*, 2004a]. If the available data is spare and does not warrant an accurate description of the FDC, then the use of an annual duration curve is advocated [*Searcy*, 1959; *Vogel and Fennessey*, 1994; *Castellarin et al.*, 2004a, b]. This curve describes the relationship between the magnitude and frequency of the streamflow for a "typical hypothetical year" [*Vogel and Fennessey*, 1994]. To construct an annual FDC, the available data is divided into n years and individual FDCs are constructed for each year. Then, for each exceedance probability a median streamflow is derived from these n different FDCs and used to create the annual FDC. *Vogel and Fennessey* [1994] used this concept to associate confidence and recurrence intervals to FDCs in a nonparametric framework. One should note that the FDC of the total data record is, in general, more accurate than the annual FDC [*Leboutillier and Waylen*, 1993].

To better analyze and understand the physical controls on the FDC, it is common practice to divide the total FDC (TFDC) into a slow (SFDC) and fast (FFDC) flow component [*Yokoo and Sivapalan*, 2011; *Cheng et al.*, 2012; *Coopersmith et al.*, 2012; *Yaeger et al.*, 2012; *Ye et al.*, 2012]. For example, *Yokoo and Sivapalan* [2011] concluded from numerical simulations with a simple water balance model that the FFDC is controlled mainly by precipitation events and timing, whereas the SFDC is most sensitive to the storage capacity of the watershed and its baseflow response. This type of analysis is of particular value in regionalization studies, and prediction in ungauged basins. Indeed, much effort

has gone towards prediction of the FDC in ungauged basins using measurements of the rainfall-runoff response from hydrologically similar, and preferably geographically nearby, gauged basins [*Holmes et al.*, 2002; *Sivapalan et al.*, 2003].

In this context, one approach has been to cluster catchments into classes with similar physiographic and climatic characteristics, and then to estimate dimensionless (non-parametric) FDCs for gauged basins which in turn are then applied to ungauged basins [*Niadas*, 2005; *Ganora et al.*, 2009]. The FDCs are normalized by an index value (e.g. mean annual runoff) to generate dimensionless curves [*Ganora et al.*, 2009]. A detailed review on methods for clustering of homogeneous catchments appears in *Sauquet and Catalogne* [2011] and *Booker and Snelder* [2012], and interested readers are referred to these publications for more information. Another approach has been to mimic the empirical (observed) FDC with a mathematical/probabilistic model and to correlate the fitting coefficients of such parametric expressions to physical and climatological characteristics of the watershed using regression techniques [*Fennessey and Vogel*, 1990; *Yu et al.*, 1996, 2002; *Croker et al.*, 2003; *Castellarin et al.*, 2004a, b, 2007; *Li et al.*, 2010; *Sauquet and Catalogne*, 2011]. Such pedotransfer functions can then be used to predict the FDC of ungauged basins from simple catchment data (e.g. soil texture, topography, vegetation cover, etc.).

Models that emulate the FDC can be grouped in two main classes: 1. Physical models that use physiographic and climatic characteristics of the watersheds (e.g. drainage area, mean areal precipitation, soil properties, etc.) as parameters of the FDC [*Singh*, 1971; *Dingman*, 1978; *Yu et al.*, 1996; *Holmes et al.*, 2002; *Yu et al.*, 2002; *Lane et al.*, 2005; *Botter et al.*, 2008; *Mohamoud*, 2008]; and, 2. Probabilistic/mathematical functions that

use between two to five fitting coefficients to mimic the empirical FDC as closely and consistently as possible [*Quimpo et al.*, 1983; *Mimikou and Kaemaki*, 1985; *Fennessey and Vogel*, 1990; *Leboutillier and Waylen*, 1993; *Franchini and Suppo*, 1996; *Cigizoglu and Bayazit*, 2000; *Croker et al.*, 2003; *Botter et al.*, 2008; *Li et al.*, 2010; *Booker and Snelder*, 2012].

The early work of *Dingman* [1978] is the first study that used physical models to mimic empirical FDCs. Topography maps were used as signature of catchment behavior to predict the FDC using relatively simple first-order polynomial functions. Two more recent studies by *Yu et al.* [1996, 2002] used similar regression functions to predict the FDC of catchments in Taiwan but considered the drainage area as main proxy of the rainfall-runoff transformation.

Probabilistic methods include the use of lognormal and lognormal mixture [*Fennessey and Vogel*, 1990; *Leboutillier and Waylen*, 1993; *Castellarin et al.*, 2004a; *Li et al.*, 2010], generalized Pareto [*Castellarin et al.*, 2004b], generalized extreme value, gamma and Gumbel [*Booker and Snelder*, 2012], beta [*Iacobellis*, 2008], and logistic distributions [*Castellarin et al.*, 2004b]. Unfortunately, the presence of temporal correlation between successive (e.g. daily) streamflow observations violates some of the basic assumptions of these classical statistical distributions, hence casting doubt on the validity of such models to describe closely and consistently the FDC [*Vogel and Fennessey*, 1994]. Other mathematical models include (amongst others) the use of exponential, power, logarithmic [*Quimpo et al.*, 1983; *Franchini and Suppo*, 1996; *Lane et al.*, 2005; *Booker and Snelder*, 2012], and polynomial functions [*Mimikou and Kaemaki*, 1985; *Yu et al.*, 2002]. In another line of work, *Cigizoglu and Bayazit* [2000] used convolution theory to predict the FDC as a product

of periodic and stochastic streamflow components. What is more, *Croker et al.* [2003] used probability theory to combine a model that predicts the FDC of days with non-zero streamflow with a distribution function that determines randomly the probability of dry days.

Notwithstanding this progress made, the probabilistic and mathematical functions used in the hydrologic literature fail, usually, to properly mimic all parts of the FDC when benchmarked against watersheds with completely different hydrologic behaviors. Consequently, some researchers focus only on a specific portion of the FDC, commonly the low flows [*Fennessey and Vogel*, 1990; *Franchini and Suppo*, 1996], whereas others prefer to use several percentiles of the FDC rather than the entire curve [*Lane et al.*, 2005; *Mohamoud*, 2008; *Blazkova and Beven*, 2009]. While complex "S" shaped FDCs can only be modeled adequately if a sufficient number of parameters (say five to seven) are used [*Ganora et al.*, 2009], one should be particularly careful using such relatively complex FDC models for regionalization and prediction in ungauged basins as parameter correlation and insensitivity can complicate and corrupt the inference and results.

In this paper, we introduce a new class of closed-form mathematical expressions which are capable of describing the FDCs of a very large number of watersheds with contrasting hydrologic behaviors. We extend the ideas presented in *Vrugt and Sadegh* [2013], and propose several commonly used functions of the soil water characteristic as mathematical models for the observed (empirical) FDCs. These models have between two to five parameters and describe closely the FDCs of the MOPEX data set. In fact, a watershed can be viewed as a large porous medium that holds and transports water depending on the soil moisture content and applied boundary conditions (rainfall and potential evapotranpira-

tion). This analogy opens up many new possibilities for analyzing the FDC and provides us with an arsenal of new mathematical expressions that can be used for (amongst others) hydrologic modeling, prediction in ungauged basins and regionalization.

This work is a follow up of *Vrugt and Sadegh* [2013] who introduced a 2-parameter formulation of the van Genuchten (VG) retention function [*van Genuchten*, 1980] as model for the FDC. The fitting coefficients of this function were derived by calibration against the observed FDC of the French Broad river basin and used as summary statistics in diagnostic model evaluation with ABC. Here, we extend this preliminary work, and introduce and benchmark several other soil water retention functions (SWRFs) using historical streamflow observations from 408 watersheds of the MOPEX data set. We are particularly interested in the quality of fit of each model, parameter sensitivity and correlation, and regionalization potential of the fitting coefficients.

The remainder of this paper is organized as follows. Section 2 provides a brief review of the most commonly used probabilistic and empirical models in the literature to mimic the FDC, and introduces several closed-form expressions of the soil water characteristic to emulate FDCs. This section also discusses the MOPEX data set, and the optimization procedure to estimate the values of the fitting coefficients of each SWRF. Then in section 3, we present and discuss the fitting results of each of the proposed parametric expressions. Here, we are especially concerned with benchmarking of our results against those of the FDC models used in the literature, analysis of parameter sensitivity and correlation, and regionalization potential of the fitting coefficients of the SWRFs. Finally, Section 4 concludes this paper with a summary of the most important findings.

2. Materials and methods

2.1. Experimental data: MOPEX data set

We use daily streamflow data from 438 MOPEX watersheds to analyze the ability of different mathematical functions to fit the empirical FDCs. This includes watersheds from across the United States with different hydrologic behaviors. The empirical FDCs are constructed using all of the available streamflow data for each watershed. Figure 1 shows the observed FDCs for eight of the MOPEX watersheds. The y-axis is scaled to a maximum value of one so that the FDCs of the watersheds can be compared more easily visually. A large variety in the FDCs of the MOPEX data set is observed. This confirms the need for a flexible function that can adequately describe the large range of hydrologic behaviors.

This rich archive of 438 catchments in the USA contains relatively long records of daily hydrologic data (rainfall, potential evapotranspiratin and streamflow). Six watersheds were excluded from our analysis due to a lack of streamflow observations, and another 24 catchments were removed due to the presence of a very large number of days with zero flow. The remaining 408 catchments have between 236 and 19,997 daily streamflow observations and were used for FDC model testing and evaluation. Obviously, a 236 day record is insufficient to warrant an accurate description of the FDC - nevertheless this data length is still appropriate for testing of the proposed models. Note, for 213 watersheds more than 54 years of daily streamflow data is available.

2.2. Probabilistic and mathematical functions

The functions most widely used in the literature to fit the observed FDCs are briefly reviewed. The skew and peakiness so clearly visible in histograms of long data records of

daily streamflow prompts the use of the Gumbel distribution to model empirical FDCs [*Booker and Snelder*, 2012]. The CDF of the Gumbel distribution is given by

$$\mathcal{F}_{\mathbf{Y}}(y_t|a_{\text{G}}, b_{\text{G}}) = \exp\left[-\exp\left(-\frac{y_t - a_{\text{G}}}{b_{\text{G}}}\right)\right], \tag{1}$$

where $\mathcal{F}_{\mathbf{X}}$ denotes the cumulative density, a_{G} signifies the location, and b_{G} measures the scale of y_t. The Gumbel distribution is a particular case of the generalized extreme value (GEV) distribution, whose CDF is given by

$$\mathcal{F}_{\mathbf{Y}}(y_t|a_{\text{GEV}}, b_{\text{GEV}}, c_{\text{GEV}}) = \exp\left(-\left[1 + c_{\text{GEV}}\left(\frac{y_t - a_{\text{GEV}}}{b_{\text{GEV}}}\right)\right]^{-1/c_{\text{GEV}}}\right), \tag{2}$$

where a_{GEV}, b_{GEV}, and c_{GEV} are the location, scale, and shape parameters, respectively. The shape parameter, c_{GEV}, controls the skewness of the distribution, and enables fitting of tailed streamflow distributions. The GEV distribution is widely used in the field of hydrology to model extremes (floods and droughts) [*Katz et al.*, 2002], as well as FDCs [*Booker and Snelder*, 2012]. Note that if $c_{\text{GEV}} = 0$, the GEV distribution simplifies to the Gumbel distribution. The exceedance probability, G_t, of a streamflow observation/simulation, y_t, can be derived from Equations 1 and 2 by simply calculating

$$G_t = 1 - \mathcal{F}_{\mathbf{Y}}(y_t|\cdot). \tag{3}$$

This concludes our description of the probabilistic models of the FDC. We continue our review with two widely used mathematical functions of the FDC, one of which is the 2-parameter exponential function of *Quimpo et al.* [1983] which is given by

$$y_t = a_{\text{Q}} \exp(-b_{\text{Q}} G_t), \tag{4}$$

where a_{Q} (mm/day) and b_{Q} (-) are fitting coefficients. This function predicts streamflow, y_t, based on exceedance probability, G_t, while the CDFs predict exceedance probability,

G_t, based on the observed discharge, y_t. We can simply invert Equation 4 to derive a mathematical expression for the exceedance probability, G_t, whose value can be compared directly against the results of Equation 3 for the probabilistic models

$$G_t = -\frac{1}{b_{\text{Q}}}\log\left(\frac{y_t}{a_{\text{Q}}}\right). \tag{5}$$

Franchini and Suppo [1996] proposed another function to model empirical FDCs. Their 3-parameter model is defined as

$$y_t = b_{\text{FS}} + a_{\text{FS}}(1 - G_t)^{c_{\text{FS}}}, \tag{6}$$

in which a_{FS} (mm/day), b_{FS} (mm/day) and c_{FS} (-) are fitting coefficients. This function was originally proposed to only fit the low flows of the FDC, but has been used to model the entire range of the FDC as well [*Sauquet and Catalogne*, 2011]. Inversion of Equation 6 provides a direct expression for the exceedance probability

$$G_t = 1 - \left(\frac{y_t - b_{\text{FS}}}{a_{\text{FS}}}\right)^{1/c_{\text{FS}}}, \tag{7}$$

so that we can compare this model against the CDF of the probabilistic models.

Practical experience suggests that the parametric models reviewed thus far are not flexible enough to warrant a close description of the FDC for all different exceedance probabilities, let alone capture adequately the large variability that exists among the FDCs of different watersheds. In the next section we introduce a new class of closed-form parametric expressions of the FDC which accurately describe the FDCs for a large range of hydrologic behaviors.

2.3. Proposed formulations

The functional shape of the FDC has many elements in common with that of the soil water characteristic. This is graphically illustrated in Figure 2 which plots the water

retention function of five different soils presented in *van Genuchten* [1980]. These curves depict the relationship between the volumetric moisture content, θ (x-axis) and the corresponding pressure head, h (y-axis) of a soil and are derived by fitting Equation

$$\theta = \theta_r + \frac{\theta_s - \theta_r}{[1 + (\alpha|h|)^n]^m} \tag{8}$$

to experimental (θ, h) data collected in the laboratory. This equation is also known as the van Genuchten (VG) model and contains five different parameters, where θ_s ($\mathrm{cm}^3/\mathrm{cm}^3$) and θ_r ($\mathrm{cm}^3/\mathrm{cm}^3$) denote the saturated and residual moisture content, respectively, and α (1/cm), n (-) and m (-) are fitting coefficients that determine the air-entry value and slope of the WRF. In most studies, the value of m is set conveniently to $1-1/n$ which not only reduces the number of parameters to four, but also provides a closed-form expression for the unsaturated soil hydraulic conductivity function [*van Genuchten*, 1980].

The shape of the WRFs plotted in Figure 2 show great similarity with the FDCs displayed previously in Figure 1. This suggests that Equation 8 might be an appropriate parametric expression for describing the functional relationship between the exceedance probability of streamflow (x-axis) and its magnitude (y-axis). To make sure that the exceedance probability is bounded exactly between 0 and 1, we set $\theta_r = 0$ and $\theta_s = 1$, respectively. This leads to the following 2-parameter VG formulation of the FDC proposed by *Vrugt and Sadegh* [2013]

$$G_t = \left[1 + (a_{\mathrm{VG}} y_t)^{\ b_{\mathrm{VG}}}\right]^{1/b_{\mathrm{VG}}-1}, \tag{9}$$

where the parameters a_{VG} (day/mm), and b_{VG} (-) need to determined by fitting against the observed FDC. If deemed appropriate, we can further increase the flexibility of Equation

238 9 by defining $c_{\text{VG}} = 1/b_{\text{VG}} - 1$. In this paper, we will test both the 2- and 3-parameter VG
239 formulations of the FDC.

The VG model is used widely in porous flow simulators to describe numerically variably saturated water flow. Yet, many other hydraulic models have been proposed in the vadose zone literature to characterize the retention and unsaturated soil hydraulic conductivity functions. We consider here the lognormal WRF of *Kosugi* [1994, 1996]

$$G_t = \begin{cases} \frac{1}{2}\,\text{erfc}\left[\frac{1}{\sqrt{2}\ b_{\text{K}}}\log\left(\frac{c_{\text{K}} - y_t}{c_{\text{K}} - a_{\text{K}}}\right)\right] & \text{if } y_t < c_{\text{K}} \\ 1 & \text{if } y_t \geq c_{\text{K}} \end{cases}, \tag{10}$$

240 where "erfc" denotes the complimentary error function, and a_{K} (mm/day), b_{K} (-) and c_{K}
241 (mm/day) are fitting coefficients that need to be determined by calibration against the
242 empirical FDC of each watershed. We can simplify this 3-parameter Kosugi formulation
243 of the FDC by setting $c_{\text{K}} = 0$. This assumption is appropriate for experimental data
244 of the soil water characteristic, and we therefore consider both the 2- and 3-parameter
245 formulations in our numerical studies with the MOPEX data set presented later.

246 The main reason to use Kosugi's WRF rather than other commonly used parametric
247 expressions of the WRF such as *Brooks and Corey* [1964], is that the parameters can be
248 related directly to the pore size distribution and hence exhibit a much better physical
249 underpinning than their counterparts of the VG model. This might increase the chances
250 of regionalization efforts.

The 2- and 3-parameter formulations of the Kosugi and VG models of the WRF assume implicitly a unimodal pore size distribution. This assumption might not be realistic for some soils and can lead to a relatively bad fit of these unimodal pore size distribution models to the observed water retention data. Soils with a heterogeneous (e.g. bimodal) pore size distribution can be much better described if we use a mixture of two or more

WRFs. We follow *Durner* [1994] and propose the following mixture FDCs for watersheds with a complex hydrologic response

$$G_t = \sum_{i=1}^{k} \left(w_{i,\mathrm{VG}} \left[1 + (a_{i,\mathrm{VG}}\, y_t)^{b_{i,\mathrm{VG}}} \right]^{1/b_{i,\mathrm{VG}}-1} \right), \tag{11}$$

$$G_t = \sum_{i=1}^{k} \left(\frac{w_{i,\mathrm{K}}}{2} \operatorname{erfc}\left[\frac{1}{\sqrt{2}\; b_{i,\mathrm{K}}} \log\left(\frac{y_t}{a_{i,\mathrm{K}}} \right) \right] \right), \tag{12}$$

where k denotes the number of constituent modes, $w_{i,\mathrm{x}}$ signifies the weight of each individual WRF ($w_{i,\mathrm{x}} \geq 0$ and $\sum_{i=1}^{k} w_{i,\mathrm{x}} = 1$), and $a_{i,\mathrm{x}}$ and $b_{i,\mathrm{x}}$ are the fitting coefficients of the ith WRF. The subscript X stands either for VG or K. If fitting of the FDC is of main importance, then one could use a relatively large value for k (e.g. $k = 5$). Yet, for diagnostic analysis and regionalization one should be particularly careful not to overfit the empirical FDCs. Indeed, considerable trade-off exists between the quality of fit of the FDC and the identifiability and correlation of the FDC model coefficients. The more parameters that are used to emulate the FDC, the better the fit to the empirical curve but at the expense of an increase in parameter uncertainty and correlation. In the present study we use $k = 2$ and hence mimic the empirical FDCs with a mixture of two VG or two Kosugi WRFs. For both classes of models, this mixture formulation has five parameters.

A bimodal FDC would seem appropriate for catchments with two or more discerning flow paths. For example, if the catchment exhibits two dominant modes (e.g. surface runoff and baseflow) then a bimodal mixture formulation of the FDC would seem appropriate. Table 1 summarizes the 2-, 3- and 5-parameter formulations of VG and Kosugi used herein to model the FDC. These models will be tested against the empirical FDCs of the MOPEX data set. These results will be presented in the next section. For completeness we have also tabulated the probabilistic models used herein.

2.4. FDC model parameter estimation

Now we have discussed the different models for the FDC (see Table 1), we are left with inference of their coefficients. We have developed a MATLAB program called FDC_Fitting which automatically determines the best values of the fitting coefficients of the FDC models used herein for a given streamflow data record. Graphical output is provided as well. FDC_Fitting implements a multi-start gradient-based local optimization approach with Levenberg Marquardt (LM) [*Marquardt*, 1963] to rapidly locate the "best" values of the FDC model parameters. A classical sum of squared error (SSE) objective function is used to summarize the distance between the observed and simulated FDCs,

$$\mathrm{SSE}(\mathbf{x}|\tilde{\mathbf{Y}}) = \sum_{t=1}^{N} \left(\tilde{G}_t - G_t(\mathbf{x}|\tilde{y}_t) \right)^2, \tag{13}$$

where $\mathbf{x}$ is the vector of fitting parameters (differs per FDC model), $\tilde{\mathbf{Y}} = \{\tilde{y}_1, \ldots, \tilde{y}_N\}$ denotes the observed streamflow data, and $\tilde{G}_t$ and G_t signify the observed and FDC modeled exceedance probabilities, respectively. To maximize LM search efficiency, the Jacobian matrix is computed using analytical expressions for $\partial G_t / \partial x_i$ ($i = \{1, \ldots, d\}$), the partial sensitivity of the output (exceedance probability) predicted by each FDC model with respect to its individual model parameters. Moreover, 20 different LM trials were used each with a different starting point, drawn randomly from $\mathcal{U}_d[0, 1]$, the d-dimensional uniform distribution on the interval between zero and one.

The LM search method is computationally efficient and much faster than global optimization methods. What is more, it does not require specification of a prior parameter space (except that all parameters are at least zero). Nevertheless, in some cases ($< 5\%$) the LM method was unable to reduce substantially the fitting errors of the (randomly chosen) starting points and the (derivative-free) Nelder-Mead Simplex algorithm [*Nelder*

and Mead, 1965] was used instead to minimize Equation 13. Numerical results for the 3- and 5-parameter VG and Kosugi FDC models demonstrate (not shown) that this hybrid two-step approach provides better results for some of the watersheds than commonly used global optimizers. This is in large part due to the rather peculiar properties of the SSE-based response surfaces (flat with one small solution pocket).

To derive explicit estimates of FDC parameter uncertainty, we also solved for the posterior distribution of the fitting coefficients using Bayesian inference with DREAM [*Vrugt et al.*, 2008, 2009]. We assume a uniform prior distribution for all the FDC parameters, and sample the target distribution by maximizing a standard Gaussian (least-squares type) log-likelihood function, $\log\big(p(\mathbf{x}|\tilde{\mathbf{Y}})\big) = -N/2\log\big(\mathrm{SSE}(\mathbf{x}|\tilde{\mathbf{Y}})\big)$ where p denotes the posterior density. In our application of DREAM, we used default settings of the algorithmic variables, and convergence of the parallel chains to a limiting distribution was assessed with different diagnostics.

3. Results and discussion

Table 2 summarizes the performance of each of the FDC models for the MOPEX data set used herein. We list separately the first (mean) and second-order (standard deviation) moment of the Root Mean Square Error (RMSE) of the fit to the empirical FDCs of the 408 different watersheds. For model selection purposes we also list the number of times (expressed in %) each respective FDC model with two, three or five parameters achieves the lowest RMSE among its constituent formulations with similar number of parameters (degrees of freedom).

The results in Table 2 highlight several key findings. Firstly, the 2-parameter FDC formulations of Kosugi and VG exhibit substantially lower mean RMSE values than their

counterparts with similar structural complexity (Gumbel, Quimpo, and Franchini and Suppo) proposed in the literature. Secondly, of the four different 2-parameter models, the Kosugi WRF is preferred for more than 60% of the watersheds as this model best fits the empirical FDCs. What is more, the two parameters of this parsimonious formulation of Kosugi exhibit a negligible correlation (shown later) which constitutes an important practical advantage for model fitting, regionalization and diagnostic model evaluation (discussed later). Thirdly, among the 3-parameter formulations of the FDC, the Kosugi, VG and GEV models exhibit a somewhat similar performance (according to RMSE), and their fit is much better than that of the model of Franchini and Suppo. Nevertheless, the Kosugi WRF is most supported by the available data as it achieves the lowest RMSE for about 56% of the catchments. Finally, the 5-parameter formulations of Kosugi and VG best fit the empirical FDCs of the MOPEX data set. The mean RMSE of these two models ranges between 0.008 - 0.009 (computed in exceedance space) and is substantially lower than values of 0.024 - 0.029 and 0.016 - 0.017 for their 2- and 3-parameter variants, respectively. Altogether, our results favor the Kosugi WRF as model for the FDC as this WRF consistently provides the closest fit to the observed FDCs (in terms of mean RMSE) for all different model complexities.

To provide more insights into the fitting results for individual catchments, consider Figure 3 that plots histograms of the RMSE values of the 408 different watersheds. The left column (A-D) plots the results for the 2-parameter FDC models, whereas the middle and right columns illustrate the results for the 3- and 5-parameter models, respectively. Color coding is used to differentiate among the FDC models. For instance, the color black in plot A, E and I refers to VG, blue in B, G, and J signifies the Kosugi model, and the

other colors (cyan, light and dark green, and gray) are used for the remaining models proposed in the literature. To simplify visual interpretation a common x-axis was used for all different models and complexities.

The results presented in Figure 3 confirm our earlier conclusions that the proposed WRF-based FDC models are superior to the probabilistic and mathematical FDC models proposed and used in the literature. For the 2-parameter functions (left column, plot B), the Kosugi model is preferred as its distribution of RMSE values is most oriented towards the left in direction of zero RMSE. The distributions of the RMSE values of the 3-parameter formulations of VG and Kosugi (plot E and F) are quite similar, and in close agreement with the histogram derived from the GEV model (plot G). These three models perform substantially better than the model of Franchini and Suppo (plot H), whose distribution of RMSE values is approximately Gaussian but with a much larger mode (about 0.08) and standard deviation. The mixture formulations of VG and Kosugi with five parameters respectively, exhibit the best overall performance. The mode of their RMSE histogram is in closest vicinity of zero and the dispersion (standard deviation) of this distribution is smallest of all different model complexities. Overall, the 5-parameter Kosugi function provides the most accurate fit to the empirical FDCs of the 408 MOPEX watersheds, and should be used if the main purpose for application of these models is solely to predict the exceedance probability for a given streamflow value.

Thus far we have focused our attention on the quality of fit of the VG and Kosugi FDC models without recourse to assessment of their parameter sensitivity, identifiability and correlation. Figure 4 plots, for a large range of streamflow values, the sensitivity of the simulated exceedance probabilities to each of the individual parameters in the VG (top

panel) and Kosugi (bottom panel) model. Color coding is used to differentiate among the different parameters of each model. We separately display the results for the 2- (left column), 3- (middle column), and 5- (right column) parameter formulations of both models. We follow *Vrugt et al.* [2002] and derive these partial sensitivities, $\partial G_t/\partial x_i$ analytically by differentiation of the VG and Kosugi WRF models to each of its parameters. For example, for the 2-parameter formulation of Kosugi, $\mathbf{x} = \{a_{\text{K}}, b_{\text{K}}\}$, the partial parameter sensitivities are given by

$$\begin{aligned} \partial G_t/\partial a_{\text{K}} &= \tfrac{1}{\sqrt{2\pi}} a_{\text{K}}^{-1} b_{\text{K}}^{-1} \exp\left(\tfrac{\log(y_t/a_{\text{K}})^2}{2b_{\text{K}}^2}\right)^{-1} \\ \partial G_t/\partial b_{\text{K}} &= \tfrac{1}{\sqrt{2\pi}} \log(y_t/a_{\text{K}}) b_{\text{K}}^{-2} \exp\left(\tfrac{\log(y_t/a_{\text{K}})^2}{2b_{\text{K}}^2}\right)^{-1}, \end{aligned} \tag{14}$$

and their numerical values are plotted in Figure 4B with a blue and red line, respectively using representative values of a_{K}, b_{K}, and $\mathbf{Y} = \{y_1, \ldots, y_N\}$. The results presented in Figure 4 highlight several important findings.

In the first place, the parameters of the VG and Kosugi FDC models appear most sensitive at lower streamflow values (0 - 10 mm/day), and are almost insensitive to high flow levels. In other words, the values of the FDC parameters are determined primarily from low and intermediate flow levels (nondriven part of the hydrograph). Secondly, parameter sensitivity decreases with increasing model complexity. This finding is most apparent for the VG model and confirms the well known trade-off that exists between quality of fit and parameter identifiability. Indeed, the more parameters that are used to fit the empirical FDCs the more difficult it becomes to constrain their values. We will revisit this topic later using Bayesian inference with DREAM. Thirdly, the parameters reach their maximum sensitivity at approximately similar streamflow values. This finding is rather unfortunate as it makes both models vulnerable to parameter correlation (interaction).

This is not particularly desirable if the fitting coefficients are used as summary statistics for diagnostic model evaluation . Finally, the partial parameter sensitivities appear jointly positive or negative (exceptions are the 3-parameter Kosugi and 5-parameter VG model) and one would therefore expect most (or all) of the parameters in each model to be correlated negatively. This can be easily verified if we consider a simple linear function with unknown slope and intercept. If we assume these two fitting coefficients to be larger than zero, then their partial sensitivities are both positive. This must induce a negative parameter correlation as an overestimation of the slope can be compensated for (somewhat) by a lower value of the intercept. A similar negative correlation is found where the slope and intercept are strictly negative. Thus if parameter uncertainty is of main concern then the 2-parameter formulations of VG and Kosugi are preferred as their fitting coefficients are most sensitive and thus best defined by fitting against the empirical FDCs.

We now provide a more detailed visual comparison of the observed and fitted FDCs. We select three watersheds with widely different rainfall-runoff response from the MOPEX data set and present their empirical FDCs in Figures 5 (Green river), 6 (Kankakee river), and 7 (Little river). The fit of the VG, Kosugi, Gumbel, Quimpo, GEV and Franchini and Suppo models is color coded and indicated with the black, blue, cyan, dark green, light green and gray lines, respectively. The top panel in each figure uses a linear scale of the observed streamflow values, whereas the bottom panel displays the results using a logarithmic scale of the flow levels. The use of these two scales helps to illuminate differences among the models. The three different columns portray the results of the 2- (left: A,D), 3- (middle: B,E), and 5- (right: C,F) parameter formulations.

The FDCs of the three different watersheds plotted in Figures 5, 6 and 7 differ quite substantially from each other. Not only in terms of the range of their streamflow observations (y-axis) but also their functional shapes. The FDCs of the Green and Little rivers appear more similar and follow closely a strongly nonlinear, banana-shaped function when plotted using a linear streamflow scale. The Kankakee watershed on the contrary has an obvious right tail, which suggests the presence of an air-entry value in WRFs. Note that all these three different FDCs become "S"-shaped when a logarithmic scale is used for the streamflow values.

Visual comparison of each of the models against the data demonstrates that the proposed WRF formulations of the FDC are in much better agreement with their measured, empirical, counterparts than the existing FDC models used in the literature. This is most obvious in the bottom panel of each Figure when a logarithmic scale is used for the streamflow values. If we focus attention to the the 2-parameter FDC models, then the Kosugi model exhibits the best overall fit. This conclusion is also supported by our findings in Table 2, which shows that for about 60% of the MOPEX watersheds the Kosugi model is superior and achieves the lowest RMSE. Although the 2-parameter VG model nicely fits the FDCs of a very large number of watersheds, this model systematically overestimates the exceedance probabilities in the left tail of the FDC curve at the higher flow levels. This deficiency is particularly noticeable for the Little river (Figure 7) and highlights a structural weakness of the VG model for watersheds with a very large number of low and high flow events and relatively few streamflow observations in between.

The flow of the Little river falls rapidly from approximately 35 to 7 mm/day, then decreases linearly to about 2 mm/day, and then smoothly reduces to values of zero.

Although the 2-parameter formulations of VG and Kosugi cannot describe perfectly the FDC of this watershed, their 5-parameter variants (Figure 7C and F) are superior and fit adequately the exceedance probabilities for the entire range of streamflow values. This finding is important as it points to the presence of two or more alternating flow regimes of the Little river watershed. Indeed, this particular watershed alternates rapidly between a relatively dry and wet state, which, in part, is caused by the temporal characteristics of the rainfall (long dry periods interrupted by short but heavy precipitation events). During the long dry periods the runoff of this basin is made up entirely of baseflow originating directly from the groundwater reservoir. This flow regime changes dramatically during a storm event when a large fraction of water is transported directly to the stream network by surface runoff. This rapid change in flow path can only be simulated adequately with a mixture of two (or more) WRFs. We conclude that if the 5-parameter formulations of the VG and Kosugi models much better fit the FDCs than their 2-, and 3-parameter formulations, the watershed likely experiences two or more alternating flow regimes.

The 3-parameter formulations of VG and Kosugi achieve a very similar fit to the data and their results can be considered nearly equivalent for these three watersheds. However, some deviations of the 3-parameter VG model are apparent at low flows (high exceedance probabilities), particularly for the Green and Little river watersheds. From the fitting results of these three watersheds we conclude that the Kosugi class of functions is best supported by the available FDC data.

We now proceed our analysis with an in-depth study of the interaction between the parameters of the WRF-based FDC formulations. Table 3 lists average linear correlation coefficients of the fitting coefficients of the VG and Kosugi models derived from MCMC

simulation with DREAM using the 408 different watersheds of the MOPEX data set. These values are calculated by computing the mean of the absolute values of the linear correlation coefficients among the posterior parameter samples of each individual watershed. Absolute values have to be used for each watershed to avoid cancellation of positive and negative correlations. Of course, strong parameter correlation is not of much importance if quality of fit is the main concern in application of the VG and Kosugi FDC models, but becomes particularly important if the fitting coefficients of each model are used as summary metrics for diagnostic analysis. Independent model parameters are also desired for regionalization studies when relating model parameters to one or more basin characteristics.

Results demonstrate that the 2-parameter formulation of Kosugi is preferred if parameter correlation is of paramount importance. The two parameters of this FDC model exhibit an average linear correlation coefficient of about 0.16. This correlation is negligibly small and of little concern for regionalization studies and diagnostic analysis. Quite interestingly, the two parameters of the VG model interact much stronger with correlation coefficient that exceeds the value of 0.8. Apparently, the 2-parameter formulation of Kosugi not only exhibits the highest qualify of fit of all models with two fitting coefficients (e.g. Table 2) but also the lowest parameter interaction. This model is preferred for diagnostic analysis and regionalization studies (discussed later).

The correlation among the fitting coefficients of the VG and Kosugi models increases significantly if the number of FDC parameters is enhanced. Indeed, for the 3- and 5-parameter variants of VG and Kosugi the correlation coefficients have increased to values of about 0.7 - 0.9 and 0.4 - 0.7, respectively. These formulations do fit better the observed

FDCs (see Table 2) but at the expense of a significant increase in parameter correlation. Quite interestingly, the correlation coefficients of the 5-parameter VG model are lower than its 3-parameter counterpart. It is not immediately obvious what causes this reduction in parameter correlation. We leave this for future studies.

Now we have determined that the Kosugi model is preferred for FDC fitting and diagnostic analysis, we now present in Figures 8 and 9 the results of our 2- and 5-parameter formulations of this model for 12 different watersheds in the USA with quite different hydrologic responses to rainfall. This includes (A) SB Potomac river, WV, (B) Tygart Valley river, WV, (C) NF Holston river, VA, (D) Little river, AR, (E) Green river, IL, (F) Kankakee river, IN, (G) EF San Gabriel river, CA, (H) White river, WA, (I) Pemigewasset river, NH, (J) Little Pee Dee river, SC, (K) Licking river, KY, and (L) Genesee river, NY. The empirical FDCs exhibit quite different functional shapes but the fit of both Kosugi formulations can be considered excellent.

Some deviations of the 2-parameter Kosugi model remain apparent at the high flows (low exceedance probabilities), particularly for semi-arid and arid watersheds that are characterized by long dry periods and occasional but large precipitation events (convective thunderstorms). Fortunately, the 5-parameter Kosugi function fits adequately these watersheds as well - in large part because of its ability to separately describe with two different WRFs the behavior of the watershed at low and high flows. The easiest watersheds to fit are those that are relatively wet (lots of precipitation) and in which the groundwater reservoir contributes a large part of the total streamflow. The FDCs of such watersheds exhibit a relatively mild slope, and this is easy to describe with just two or

three parameters. Examples includes the Kankakee (F), White (H), and Little Pee Dee (J) river basins.

We now focus our attention on model uncertainty, and on the 95% ranges of the 5-parameter Kosugi model for the (A) SB Potomac, (B) Tygart Valley, (C) NF Holston, (D) Little, (E) Green, (F) Kankakee, (G) EF San Gabriel, (H) White, (I) Pemigewasset, (J) Little Pee Dee, (K) Licking, and (L) Genesee river basins. We plot separately the effects of parameter (dark gray) and model (light gray) uncertainty in Figure 10. The fit to the data is excellent and this makes it difficult to visualize clearly the results. The parameter and total model uncertainty is rather small, and almost covered completely by the data of the empirical FDCs of each watershed. The exception to this are the NF Holston (C), Little (D), and Genesee (L) river basins. The simulation uncertainty ranges are somewhat larger as the empirical FDCs are not fitted perfectly close at all times. Indeed, the 95% parameter uncertainty is clearly visible in plots (C) and (L) and show the small deviation of the fitted function from the empirical FDC.

The 2-parameter lognormal WRF model of Kosugi has the advantage that its parameters can be directly related to the pore size distribution. In other words, the parameters should have a physical interpretation. We verify this and calculate the linear correlation coefficients between the five parameters of the Kosugi model and the MOPEX basin characteristics. Correlations are relatively low and range between values of $r = -0.5$ and $r = 0.5$. The two parameters of the original Kosugi function, however, show a much higher correlation with the physical and climatic characteristics of the watersheds. For instance, our analysis demonstrates that the parameters a_{κ} and b_{κ} are most related to climatic variables (mean annual precipitation and potential evapotranspiration) and

reach linear correlation coefficients of approximately 0.8. This opens up new possibilities for regionalization and prediction in ungaged basins using for instance, remote sensing precipitation data products.

We conclude the results section with some final remarks: (1) The fitting of the proposed FDC models is not without problems. We therefore recommend to use different starting points with a local search method to minimize chances of premature convergence to the wrong values of the FDC fitting coefficients, and (2) The proposed WRF-based functions demonstrate low sensitivity to high flows (Figure 4), and hence some care should be exercised if these models are used to estimate the exceedance probability of extreme events. One way to mitigate this problem is to define the objective function of Equation 13 in the streamflow space rather than exceedance probability space. This would require the functions of Table 1 to be inverted so that they predict the streamflow value, y_t for each observed exceedance probability, G_t.

4. Conclusions

The FDC has been used to characterize information regarding catchment streamflow variability and flow regime in various hydrologic design and management studies. While several physically-based and probabilistic/mathematical functions have been used to model the empirical FDCs, they fail to characterize adequately the mid-section and tails of the FDC at low and high exceedance probabilities, respectively, and the large differences between the FDCs of watersheds with contrasting hydrologic behaviors. This paper extends the work of *Vrugt and Sadegh* [2013] and introduces a new class of closed-form parametric expressions to closely characterize the FDCs of arid, semi-arid, and wet catchments. These continuous functions, equivalent to the WRFs of VG and Kosugi, are

519 derived from the field of vadose zone hydrology and have been used widely to describe
520 the water characteristic of variably saturated soils. Three different formulations of the
521 VG and Kosugi models have been introduced to mimic empirical FDCs. These functions
522 differ in their structural complexity and include between two to five coefficients whose
523 values need to be derived by fitting against the observed FDCs.

524 Application of the WRFs to 408 watersheds of the MOPEX data set demonstrates that
525 the VG and Kosugi models closely match the empirical FDCs of arid, semi-arid, and wet
526 catchments. The proposed parametric expressions exhibit a superior performance over
527 commonly used FDC models in the hydrologic literature. If quality of fit is of paramount
528 importance then the 5-parameter Kosugi model is preferred as it provides the closest fit
529 to the empirical FDCs. What is more, this mixture formulation of two WRFs can help to
530 discern different stable states of the catchment. If the fitting coefficients of the FDC model
531 are to be used for regionalization or as summary statistics in diagnostic analysis then the
532 2-parameter formulation of Kosugi is preferred. The parameters of this model exhibit
533 a negligibly small correlation and are therefore suitable metrics that are well defined
534 by calibration against the observed FDCs. We conclude that a maximum of four-five
535 parameters is sufficient to describe the large range of FDCs of the MOPEX data set.

536 **Acknowledgments.** The first and second author appreciate the support and fund-
537 ing from the UC-Lab Fees Research Program Award 237825. The MATLAB code of
538 FDC_Fitting can be obtained from the second author upon request, (jasper@uci.edu).
539 The MOPEX watersheds' data was obtained from NOAA's national weather service web
540 page available at ftp://hydrology.nws.noaa.gov/pub/gcip/mopex/US_Data/.

References

Alaouze, C.M. (1989), Reservoir releases to uses with different reliability requirements, *Water Resources Bulletin*, *25*(6),1163–1168.

Assouline, S., D. Tessier, and A. Bruand (1998), A conceptual model of the soil water retention curve, *Water Resour. Res.*, *34*(2), 223-231.

Blazkova, S., and K. Beven (2009), A limits of acceptability approach to model evaluation and uncertainty estimation in flood frequency estimation by continuous simulation: Skalka catchment, Czech Republic, *Water Resour. Res.*, *45*, W00B16, doi:10.1029/2007WR006726.

Booker, D.J., and T.H. Snelder (2012), Comparing methods for estimating flow duration curves at ungauged sites, *Journal of Hydrology*, *434-435*, 78–94.

Botter, G., S. Zanardo, A. Porporato, I. Rodriguez-Iturbe, A. and Rinaldo (2008), Ecohydrological model of flow duration curves and annual minima, *Water Resources Research*, *44*, W08418, doi:10.1029/2008WR006814.

Brooks, R.H., and A.T. Corey (1964), Hydraulic properties of porous media, Hydrol. Pap. 3, Colo. State Univ., Fort Collins.

Burke, E.J., R.H.J. Perry, S.J. Brown (2010), An extreme value analysis of UK drought and projections of change in the future, *Journal of Hydrology*, *388*(131), doi:10.1016/j.jhydrol.2010.04.035.

Castellarin, A., G. Galeati, L. Brandimarte, A. Montanari, and A. Brath (2004a), Regional flow-duration curves: reliability for ungauged basins, *Advances in Water Resources*, *27*, 953–965.

562 Castellarin, A., R.M. Vogel, and A. Brath (2004b), A stochastic index flow model of flow
563 duration curves, *Water Resources Research*, *40*, W03104, doi:10.1029/2003WR002524.
564 Castellarin, A., G. Camorani, and A. Brath (2007), Predicting annual and long-
565 term flow-duration curves in ungauged basins, *Adv. Water Resour.*, *30*, 937–953,
566 doi:10.1016/j.advwatres.2006.08.006.
567 Cheng, L., M. Yaeger, A. Viglione, E. Coopersmith, S. Ye, and M. Sivapalan (2012), Ex-
568 ploring the physical controls of regional patterns of flow duration curves Part 1: Insights
569 from statistical analyses, *Hydrol. Earth Syst. Sci.*, *16*, 4435-4446, doi:10.5194/hess-16-
570 4435-2012.
571 Chow, V.T. (1964), Handbook of applied hydrology, Mc-Graw Hill BookCo., New York,
572 N.Y.
573 Cigizoglu, H.K., and M. Bayazit (2000), A generalized seasonal model for flow duration
574 curve, *Hydrol. Process.*, *14*, 1053–1067.
575 Cole, R.A.J., H.T. Johnston, and D.J. Robinson (2003), The use of flow duration curves
576 as a data quality tool, *Hydrological Sciences Journal*, *48*(6), 939–951.
577 Coopersmith, E., M.A. Yaeger, S. Ye, L. Cheng, and M. Sivapalan (2012), Exploring the
578 physical controls of regional patterns of flow duration curves Part 3: A catchment
579 classification system based on regime curve indicators, *Hydrol. Earth Syst. Sci.*, *16*,
580 4467-4482, doi:10.5194/hess-16-4467-2012.
581 Croker, K.M., A.R. Young, M.D. Zaidman, and H.G. Rees (2003), Flow duration curve
582 estimation in ephemeral catchments in Portugal, *Hydrological Sciences Journal*, *48*(3),
583 427–439, DOI: 10.1623/hysj.48.3.427.45287.

584 Dingman, S.L. (1978), Sythesis of Flow-Duration Curves for Unregulated Streams in New
585 Hampshire, *Water Resources Boulletin*, *14*(6), 1481–1502.

586 Duan, Q., S. Sorooshian, V.K. Gupta (1994), Optimal use of the SCE-UA global op-
587 timization method for calibrating watershed models, *Journal of Hydrology*, *158*(3-4),
588 265–284.

589 Durner, W. (1994), Hydraulic conductivity estimation for soils with heterogeneous pore
590 structure, *Water Resources Research*, *30*(2), 211–223.

591 Euser, T., H.C. Winsemius, M. Hrachowitz, F. Fenicia, S. Uhlenbrook, and H.H.G.
592 Savenije (2013), A framework to assess the realism of model structures using hydrolog-
593 ical signatures, *Hydrol. Earth Syst. Sci.*, *17*, 1893–1912, doi:10.5194/hess-17-1893-2013.

594 Fennessey, N., and R.M. Vogel (1990), Regional Flow-Duration Curves for Ungauged Sites
595 in Massachusetts, *J. Water Resour. Plann. Manage.*, *116*, 530–549.

596 Foster, H.A (1934) Duration curves, *ASCE Transactions*, *99*, 1213–1267.

597 Franchini, M. and M. Suppo (1996), Regional analysis of flow duration curves for a lime-
598 stone region, *Water Resour. Manage.*, *10*, 199-218.

599 Ganora, D., P. Claps, F. Laio, and A. Viglione (2009), An approach to estimate non-
600 parametric flow duration curves in ungauged basins, *Water Resour. Res.*, *45*, W10418,
601 doi:10.1029/2008WR007472.

602 Gupta, H.V., T. Wagener, and Y. Liu (2008), Reconciling theory with observations: el-
603 ements of a diagnostic approach to model evaluation, *Hydrological Processes*, *22*(18),
604 3802–3813.

605 Gupta, H.V., M.P. Clark, J.A. Vrugt, G. Abramowitz, and M. Ye (2012), Towards a com-
606 prehensive assessment of model structural adequacy, *Water Resour. Res.*, *48*, W08301,

607 doi:10.1029/2011WR011044.

608 Haan, C.T. (1977), Statistical Methods in Hydrology, Iowa State University Press, Ames.

609 Holmes, M.G.R., A.R. Young, A. Gustard, and R. Grew (2002), A region of influence
610 approach to predicting flow duration curves within ungauged catchments, *Hydrol. Earth*
611 *Syst. Sci.*, *6*, 721-731, doi:10.5194/hess-6-721-2002.

612 Hughes, D.A., and V. Smakhtin (1996), Daily flow time series patching or extension:
613 a spatial interpolation approach based on flow duration curves, *Hydrological Sciences*
614 *Journal*, *41*(6), 851-871, doi: 10.1080/02626669609491555.

615 Iacobellis, V. (2008), Probabilistic model for the estimation of T year flow duration curves,
616 *Water Resour. Res.*, *44*, W02413, doi:10.1029/2006WR005400.

617 Jehng-Jung, K., and S.F. Bau (1996), Risk Analysis for Flow Duration Curve Based
618 Seasonal Discharge Management Programs, *Wat. Res.*, *30*(6), 1369–1376.

619 Katz, R.W., M.B. Parlange, P. Naveau (2002), Statistics of extremes in hydrology, *Ad-*
620 *vances in Water Resources*, *25*(812), 1287–1304.

621 Kavetski, D., F. Fenicia, and M.P. Clark (2011), Impact of temporal data resolution
622 on parameter inference and model identification in conceptual hydrological model-
623 ing: Insights from an experimental catchment, *Water Resour. Res.*, *47*, W05501,
624 doi:10.1029/2010WR009525.

625 Kosugi, K. (1994), Three-parameter lognormal distribution model for soil water retention,
626 *Water Resources Research*, *30*(4), 891–901.

627 Kosugi, K. (1996), Lognormal distribution model for unsaturated soil hydraulic properties,
628 *Water Resources Research*, *32*(9), 2697–2703.

Kunkle, G.R. (1962), The Baseflow-Duration Curve, a Technique for the study of Groundwater Discharge from a Drainage Basin, *Journal of Geophysical Research*, *67*(4), 1543–1554.

Lagarias, J.C., J.A. Reeds, M.H. Wright, and P.E. Wright (1998), Convergence Properties of the Nelder-Mead Simplex Method in Low Dimensions, *SIAM Journal of Optimization*, *9*(1), 112–147.

Lane, P.N.J., A.E. Best, K. Hickel, and L. Zhang (2005), The response of flow duration curves to afforestation, *Journal of Hydrology*, *310*, 253–265.

Leboutillier, D.W., and P.R. Waylen (1993), A Stochastic Model of Flow Duration Curves, *Water Resources Research*, *29*(10), 3535–3541.

Li, M., Q. Shao, L. Zhang, and F.H.S. Chiew (2010), A new regionalization approach and its application to predict flow duration curve in ungauged basins, *J. Hydrol.*, *389*(12), 137–145.

Male, J.W., and H. Ogawa (1984), Tradeoffs in water quality management, *Water Resources Planning and Management*, *110*(4), 434–444.

Mallory, S.J.L., and R.S. McKenzie (1993), Water resources modeling of flow diversions. *Proceedings of the Sixth South African National Hydrology Symposium, Pietermaritzburg, South Africa*, *1*, 429–436.

Marquardt, D. (1963), An algorithm for least-squares estimation of nonlinear parameters, *Journal of the Society of Industrial and Applied Mathematics*, *11*(2), 431–441.

Masih, I., S. Uhlenbrook, S. Maskey, M.D. Ahmad (2010), Regionalization of a conceptual rainfallrunoff model based on similarity of the flow duration curve: A case study from the semi-arid Karkheh basin, Iran, *Journal of Hydrology*, *391*, 188–201.

652 Mimikou, M., and S. Kaemaki (1985), Regionalization of Flow Duration Characteristics,
653 *Journal of Hydrology*, *82*, 77–91.

654 Mitchell, W.D. (1957), Flow duration curves of Illinois streams, Illinois Department of
655 Public Works and Buildings, Division of Waterways.

656 Mohamoud, Y. M. (2008), Prediction of daily flow duration curve and streamflow for
657 ungauged catchments using regional flow duration curves, *Hydrolog. Sci. J.*, *53*, 706–
658 724, doi:10.1623/hysj.53.4.706.

659 Mohanty, B.P., R.S. Bowman, J.M.H. Hendrickx, and M.T. van Genuchten (1997),
660 New piecewise-continuous hydraulic functions for modeling preferential flow in an
661 intermittent-flood-irrigated field, *Water Resources Research*, *33*(9), 2049–1063.

662 Nelder, J.A., and R. Mead (1965), A simplex method for function minimization, *Computer*
663 *Journal*, *7*, 308–313.

664 Niadas, I.A. (2005), Regional flow duration curve estimation in small ungauged catch-
665 ments using instantaneous flow measurements and a censored data approach, *Journal*
666 *of Hydrology*, *314*, 48–66.

667 Pfannerstill, M., B. Guse, and N. Fohrer (2014), Smart low flow signature metrics for an
668 improved overall performance evaluation of hydrological models, *Journal of Hydrology*,
669 *510*, 447–458.

670 Pitman, W.V. (1993), Simulation of run-of-river schemes using monthly data, *Proceedings*
671 *of the Sixth South African Hydrology Symposium, Pietermarietzburg, South Africa*, *1*,
672 445–452.

673 Quimpo, R.G., A.A. Alejandrino, and T.A. McNally (1983) Regionalised flow duration
674 curves for Philippines, *Journal of Water Resources Planning and Management*, *109*(4),

675 320330.

676 Refsgaard, J.C. and J. Knudsen (1996), Operational validation and intercomparison of
677 different types of hydrological models, *Water Resour. Res.*, *32*, 21892202.

678 Sadegh, M., and J.A. Vrugt (2014a), Approximate Bayesian Computation using Markov
679 Chain Monte Carlo simulation: DREAM$_{(\mathrm{ABC})}$, *Water Resour. Res.*, *50*, 67676787,
680 doi:10.1002/2014WR015386, 2014a.

681 Sadegh, M., J.A. Vrugt, C. Xu, and E. Volpi (2014b), Diagnosing Nonstationary Wa-
682 tershed Behavior from Process-Based Model Evaluation using Approximate Bayesian
683 Computation, *Water Resources Research*, under review, 2014b.

684 Sauquet, E., and C. Catalogne (2011), Comparison of catchment grouping methods for
685 flow duration curve estimation at ungauged sites in France, *Hydrol. Earth Syst. Sci.*,
686 *15*, 2421-2435.

687 Savicz, K., T. Wagener, M. Sivapalan, P.A. Troch, and G. Carrillo (2011), Catchment
688 classification: empirical analysis of hydrologic similarity based on catchment function
689 in the eastern USA, *Hydrology and Earth System Sciences*, *15*, 2895–2911.

690 Schaefli, B., and H.V. Gupta (2007), Do Nash values have value?, *Hydrol. Processes*, *21*,
691 2075–2080.

692 Searcy, J.K. (1959), Flow-duration curves, Water Supply Paper 1542-A, U.S. Geological
693 Survey, Reston, Virginia,.

694 Singh, K. P. (1971), Model flow duration and streamflow variability, *Water Resour. Res.*,
695 *7*(4), 1031–1036.

696 Singh, R.D., S.K. Mishra, and H. Chowdhary (2001), Regional flow-duration models for
697 large number of ungauged Himalayan catchments for planning microhydro projects, *J.*

Hydrol. Eng., *6*(4), 310–316.

Sivapalan, M., K. Takeuchi, S.W. Franks, V.K. Gupta, H. Karambiri, V. Lakshmi, X. Liang, J.J. McDonnell, E.M. Mendiondo, P. E. O'Connell, T. Oki, J.W. Pomeroy, D. Schertzer, S. Uhlenbrook, and E. Zehe (2003), IAHS decade on predictions in ungauged basins (PUB), 20032012: Shaping an exciting future for the hydrological sciences, *Hydrolog. Sci. J.*, *48*, 857–880, doi:10.1623/hysj.48.6.857.51421.

Smakhtin, V. U. (2001), Low flow hydrology: a review, *J. Hydrol.*, *240*, 147–186.

Son, K. and M. Sivapalan (2007), Improving model structure and reducing parameter uncertainty in conceptual water balance models through the use of auxiliary data, *Water Resour. Res.*, *43*, W01415, doi:01410.01029/02006wr005032.

Tharme, R.E. (2003), A global perspective on environmental flow assessment: emerging trends in the development and application of environmental flow methodologies for rivers, *River Res. Appl.*, *19*, 397-441, doi:10.1002/rra.736.

van Genuchten, M.T. (1980) A closed-form equation for predicting the hydraulic conductivity of unsaturated soils, *Soil Science Society of America Journal*, *44*(5), 892–898.

Vogel, R.M., and N.M. Fennessey (1994), Flow-duration curves I: New interpretation and confidence intervals, *Journal of Water Resources Planning and Management*, *120*(4), 485–504.

Vogel, R.M., and N.M. Fennessey (1995), Flow-duration curves II: A Review of applications in water resources planning, *Water Resour. Bull.*, *31*(6), 1029–1039.

Vrugt, J.A., W. Bouten, H.V. Gupta, and S. Sorooshian (2002), Toward improved identifiability of hydrologic model parameters: The information content of experimental data, *Water Resour. Res.*, *38*(12), 1312, doi:10.1029/2001WR001118.

721 Vrugt, J.A., C.J.F. ter Braak, H.V. Gupta, and B.A. Robinson (2008), Equifinality
722 of formal (DREAM) and informal (GLUE) Bayesian approaches in hydrologic mod-
723 eling?, *Stochastic Environmental Research and Risk Assessment, 23(7)*, 1011–1026,
724 doi:10.1007/s00477-008-0274-y.

725 Vrugt, J.A., C.J.F. ter Braak, C.G.H. Diks, D. Higdon, B.A. Robinson, and J.M. Hyman
726 (2009), Accelerating Markov chain Monte Carlo simulation by differential evolution
727 with self-adaptive randomized subspace sampling, *International Journal of Nonlinear*
728 *Sciences and Numerical Simulation*, *10*(3), 273–290.

729 Vrugt, J.A. and M. Sadegh (2013), Toward diagnostic model calibration and evalu-
730 ation: Approximate Bayesian Computation, *Water Resources Research*, *49*, 1–11,
731 doi:10.1002/wrcr.20354.

732 Wagener, T., and H.S. Wheater (2006), Parameter estimation and regionalization for
733 continuous rainfall-runoff models including uncertainty, *Journal of Hydrology*, *320*, 132–
734 154.

735 Warnick, C.C. (1984), Hydropower engineering, Prentice-Hall, Inc., Englewood Cliffs,
736 New Jersey, 59–73.

737 Westerberg, I. K., J.-L. Guerrero, P.M. Younger, K.J. Beven, J. Seibert, S. Halldin, J.E.
738 Freer, and C.-Y. Xu (2011), Calibration of hydrological models using flow-duration
739 curves, *Hydrol. Earth Syst. Sci.*, *15*, 22052227, doi:10.5194/hess-15-2205-2011.

740 Wilby, R., B. Greenfield, and C. Glenny (1994), A coupled synoptichydrological model
741 for climate change impact assessment, *J. Hydrol.*, 153, 265–290.

742 Yadav, M., T. Wagener, and H. Gupta (2007), Regionalization of constraints on expected
743 watershed response, *Adv. Water Resour.*, *30*, 1756–1774.

744 Yaeger, M., E. Coopersmith, S. Ye, L. Cheng, A. Viglione, and M. Sivapalan (2012),
745 Exploring the physical controls of regional patterns of flow duration curves Part 4: A
746 synthesis of empirical analysis, process modeling and catchment classification, *Hydrol.*
747 *Earth Syst. Sci.*, *16*, 44834498, doi:10.5194/hess-16-4483- 2012.
748 Ye, S., M. Yaeger, E. Coopersmith, L. Cheng, and M. Sivapalan (2012), Exploring the
749 physical controls of regional patterns of flow duration curves Part 2: Role of seasonality,
750 the regime curve, and associated process controls, *Hydrol. Earth Syst. Sci.*, *16*, 4447–
751 4465, doi:10.5194/hess-16-4447-2012.
752 Yilmaz, K., H.V. Gupta, and T. Wagener (2008), A process-based diagnostic approach
753 to model evaluation: Application to the NWS distributed hydrologic model, *Water*
754 *Resour. Res.*, *44*, W09417, doi:10.1029/2007WR006716.
755 Yokoo, Y. and M. Sivapalan (2011), Towards reconstruction of the flow duration curve:
756 development of a conceptual framework with a physical basis, *Hydrol. Earth Syst. Sci.*,
757 *15*, 28052819, doi:10.5194/hess-15-2805-2011.
758 Yu, P.S., and T.C. Yang (1996), Synthetic regional flow duration curve for southern
759 Taiwan, *Hydrolog. Process.*, *10*, 373391.
760 Yu, P.S. and T.C. Yang (2000), Using synthetic flow duration curves for rainfall-runoff
761 model calibration at ungauged sites, *Hydrol. Process.*, *14*, 117–133.
762 Yu, P.S., T.C. Yang, and Y.C. Wang (2002), Uncertainty analysis of regional flow duration
763 curves, *J. Water Resour. Pl. Manage.*, *128*(6), 424–430.
764 Zhang, L., N. Potter, K. Hickel, Y. Zhang, and Q. Shao (2008), Water balance modeling
765 over variable time scales based on the Budyko framework Model development and
766 testing, *J. Hydrol.*, *360*, 117131, doi:10.1016/j.jhydrol.2008.07.021.

767 Zhao, F., Z. Xu and L. Zhang (2012), Changes in streamflow regime following vegetation
768 changes from paired catchments, *Hydrol. Process.*, *26*, 1561–1573, doi:10.1002/hyp.8266.

Table 1. Summary of the probablistic, mathematical and WRF-based functions of the FDC. All these functions compute the exceedance probability, G_t for a given streamflow value, y_t. The variables a, b, and c are fitting coefficients whose values need to be derived by calibration against the observed, empirical, FDC of individual watersheds.

Model name	Model formulation
	2-parameter formulations
Gumbel	$G_t = 1 - \exp\left[-\exp\left(-\frac{y_t - a_{\mathrm{G}}}{b_{\mathrm{G}}}\right)\right]$
Quimpo	$G_t = -\frac{1}{b_{\mathrm{Q}}}\log\left(\frac{y_t}{a_{\mathrm{Q}}}\right)$
VG	$G_t = \left[1 + (a_{\mathrm{VG}} y_t)^{b_{\mathrm{VG}}}\right]^{1/b_{\mathrm{VG}}-1}$
Kosugi	$G_t = \frac{1}{2}\,\mathrm{erfc}\left[\frac{1}{\sqrt{2}\ b_{\mathrm{K}}}\log\left(\frac{y_t}{a_{\mathrm{K}}}\right)\right]$
	3-parameter formulations
GEV	$G_t = 1 - \exp\left(-\left[1 + c_{\mathrm{GEV}}\left(\frac{y_t - a_{\mathrm{GEV}}}{b_{\mathrm{GEV}}}\right)\right]^{-1/c_{\mathrm{GEV}}}\right)$
Franchini and Suppo	$G_t = 1 - \left(\frac{y_t - b_{\mathrm{FS}}}{a_{\mathrm{FS}}}\right)^{1/c_{\mathrm{FS}}}$
VG	$G_t = \left[1 + (a_{\mathrm{VG}} y_t)\ b_{\mathrm{VG}}\right]^{-c_{\mathrm{VG}}}$
Kosugi	$G_t = \begin{cases} \frac{1}{2}\,\mathrm{erfc}\left[\frac{1}{\sqrt{2}\ b_{\mathrm{K}}}\log\left(\frac{c_{\mathrm{K}} - y_t}{c_{\mathrm{K}} - a_{\mathrm{K}}}\right)\right] & \text{if } y_t < c_{\mathrm{K}} \\ 1 & \text{if } y_t \geq c_{\mathrm{K}} \end{cases}$
	5-parameter formulations
VG	$G_t = \sum_{i=1}^{2}\left(w_{i,\mathrm{VG}}\left[1 + (a_{i,\mathrm{VG}} y_t)^{b_{i,\mathrm{VG}}}\right]^{1/b_{i,\mathrm{VG}}-1}\right)$
Kosugi	$G_t = \sum_{i=1}^{2}\left(\frac{w_{i,\mathrm{K}}}{2}\,\mathrm{erfc}\left[\frac{1}{\sqrt{2}\ b_{i,\mathrm{K}}}\log\left(\frac{y_t}{a_{i,\mathrm{K}}}\right)\right]\right)$

Table 2. Performance statistics of the quality of fit of each individual FDC model. We list the mean and standard deviation of the Root Mean Square Error (RMSE) (derived from Equation 13), and the number of times (in %) each respective model within a certain parametric class provides the best fit (lowest RMSE) to the observed FDCs.

Model name	Mean RMSE	STD of RMSE	% Best model
2-parameter formulations			
Gumbel	0.093	0.016	0
Quimpo	0.066	0.026	0.7
VG	0.026	0.012	39.2
Kosugi	0.021	0.014	60.1
3-parameter formulations			
GEV	0.015	0.008	9.8
Franchini and Suppo	0.081	0.021	0.3
VG	0.014	0.007	30.6
Kosugi	0.013	0.008	59.3
5-parameter formulations			
VG	0.006	0.003	30.9
Kosugi	0.005	0.003	69.1

Table 3. Average linear correlation coefficients of the DREAM-derived posterior parameter samples for the 408 different watersheds of the MOPEX data set. The variable "X" that is used in subscript stands for K or VG respectively.

	2-parameter formulations			
	a_{VG}	b_{VG}	a_{K}	b_{K}
a_{x}	1.00	0.81	1.00	0.16
b_{x}	0.81	1.00	0.16	1.00

	3-parameter formulations					
	a_{VG}	b_{VG}	c_{VG}	a_{K}	b_{K}	c_{K}
a_{x}	1.00	0.89	0.96	1.00	0.44	0.46
b_{x}	0.89	1.00	0.93	0.44	1.00	0.67
c_{x}	0.96	0.93	1.00	0.46	0.67	1.00

	5-parameter formulations									
	$a_{1,\mathrm{VG}}$	$b_{1,\mathrm{VG}}$	$a_{2,\mathrm{VG}}$	$b_{2,\mathrm{VG}}$	$w_{1,\mathrm{VG}}$	$a_{1,\mathrm{K}}$	$b_{1,\mathrm{K}}$	$a_{2,\mathrm{K}}$	$b_{2,\mathrm{K}}$	$w_{1,\mathrm{K}}$
$a_{1,\mathrm{x}}$	1.00	0.73	0.73	0.64	0.79	1.00	0.73	0.72	0.69	0.76
$b_{1,\mathrm{x}}$	0.73	1.00	0.65	0.62	0.77	0.73	1.00	0.69	0.62	0.70
$a_{2,\mathrm{x}}$	0.73	0.65	1.00	0.71	0.79	0.72	0.69	1.00	0.71	0.74
$b_{2,\mathrm{x}}$	0.64	0.62	0.71	1.00	0.75	0.69	0.62	0.71	1.00	0.69
$w_{1,\mathrm{x}}$	0.79	0.77	0.79	0.75	1.00	0.76	0.70	0.74	0.69	1.00

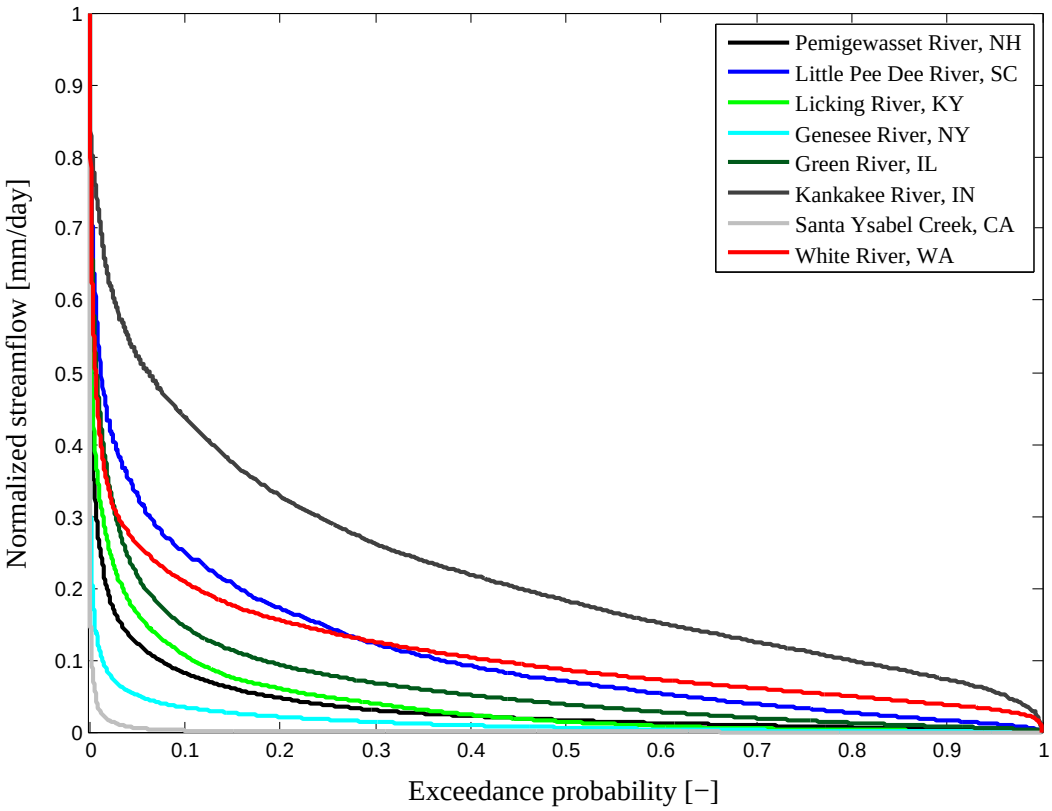

Figure 1. Flow duration curves for eight watersheds from the MOPEX data set, which show contrasting hydrologic behaviors. This figure plots normalized streamflows (mm/day) versus exceedance probability (-). We normalized the streamflow values to plot various shapes of the FDCs in one figure.

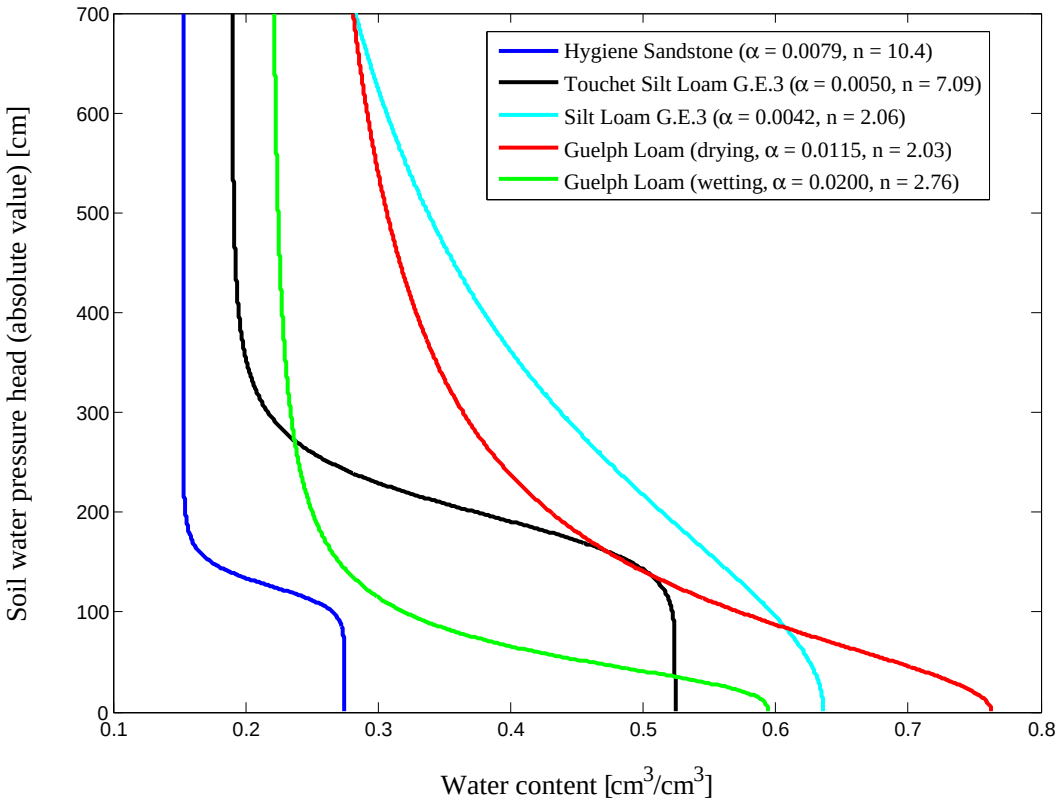

Figure 2. Water retention curves for five different soil types introduced in *van Genuchten* [1980]. This figure plots soil water pressure head (cm) versus soil water content (cm^3/cm^3). Note that the soil water pressure head values are originally negative, but we use positive pressure heads for plotting since the absolute values are used in the WRFs.

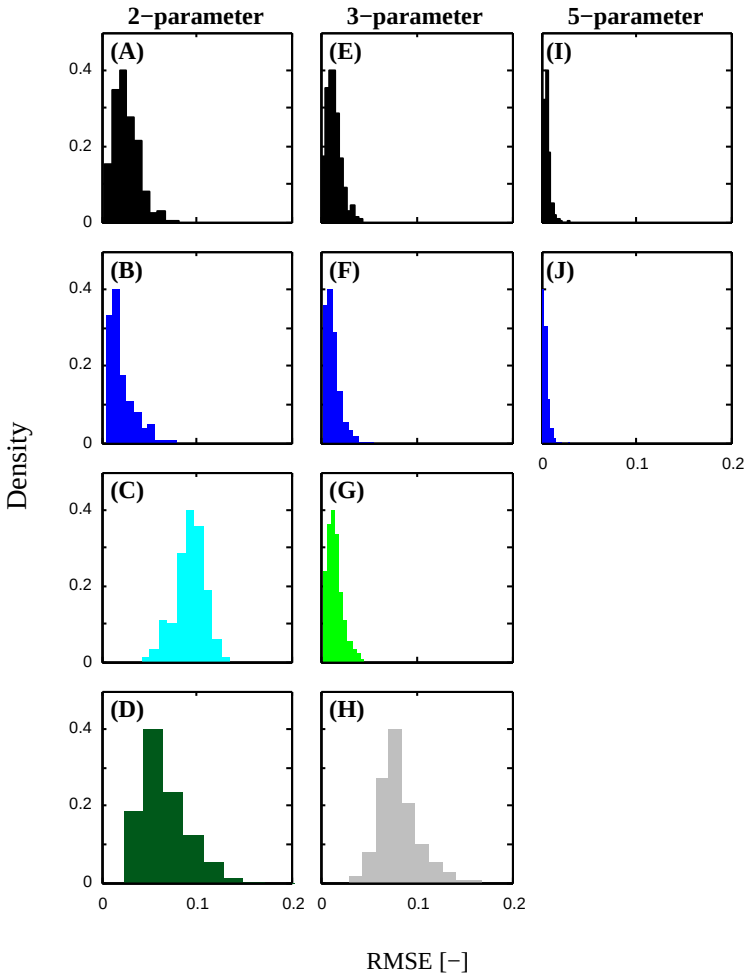

Figure 3. Histogram of the root mean square errors (RMSEs) between the simulated and observed FDCs for the 408 studied watersheds. The x-axis in each plot represents the RMSE values (dimensionless) and the y-axis shows the density of the number of occurrences for each RMSE value. Left, middle and right columns show the results of 2-, 3-, and 5-parameter model formulations, respectively. The results of the VG (plots: A, E, I), Kosugi (plots: B, F, J), Gumbel (plot: C), Quimpo (plot: D), GEV (plot: G), and Franchini and Suppo (plot: H) are presented with black, blue, cyan, dark green, light green, and gray bins, respectively. The RMSE shows the deviation between the simulated and empirical exceedance probabilities, and is hence dimensionless.

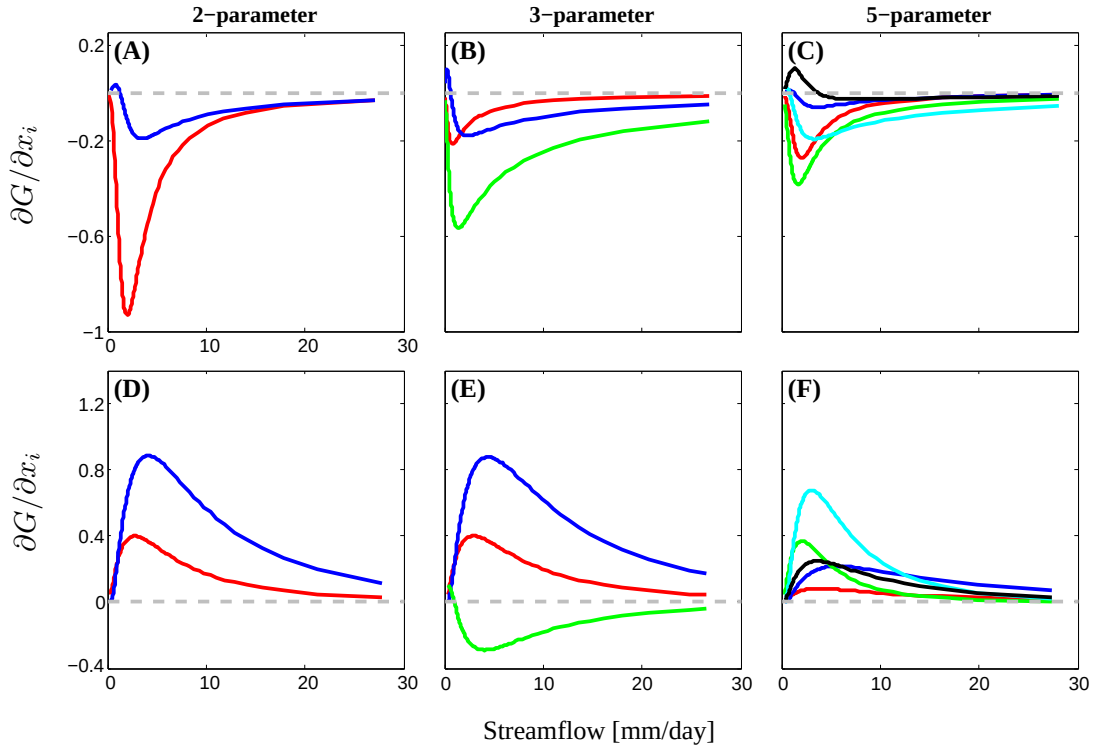

Figure 4. Partial parameter sensitivities of the VG (top panel) and Kosugi (bottom panel) models of the FDC (see Table 1) for a range of different streamflow values. Color coding is used to discern between the parameters a_{x} and $a_{1,\mathrm{x}}$ (red), b_{x} and $b_{1,\mathrm{x}}$ (blue), c_{x} and $a_{2,\mathrm{x}}$ (green), $b_{2,\mathrm{x}}$ (cyan), and $w_{1,\mathrm{x}}$ (black) of the different model formulations. The subscript X stands for VG and K. To help with visual interpretation, the gray dashed line depicts, for all flow levels, a zero sensitivity.

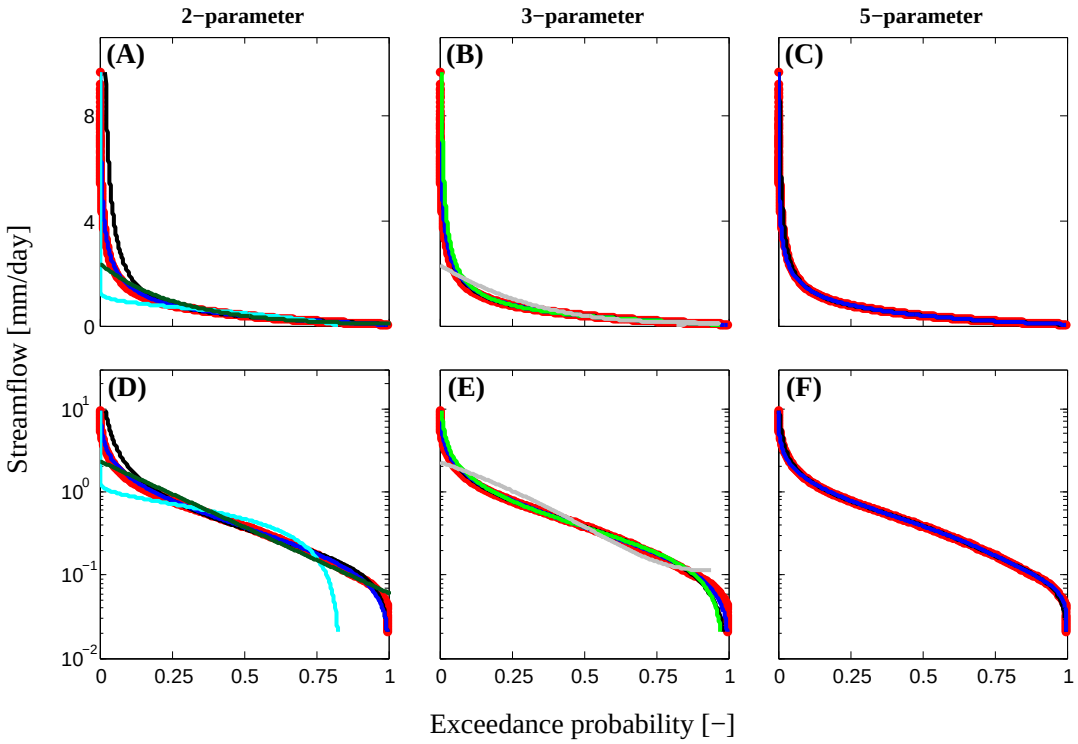

Figure 5. Comparison of the observed (red dots) and fitted (different lines) FDCs of the Green river watershed near Genesco, IL, USA. The top (A-C) panel uses a linear scale of the streamflow values, whereas the bottom (D-F) panel uses a logarithmic scale. The different columns represent different model complexities. Color coding is used to differentiate between the FDC models of Table 1: VG (black), Kosugi (blue), Gumbel (cyan), Quimpo (dark green), GEV (light green) and Franchini and Suppo (gray).

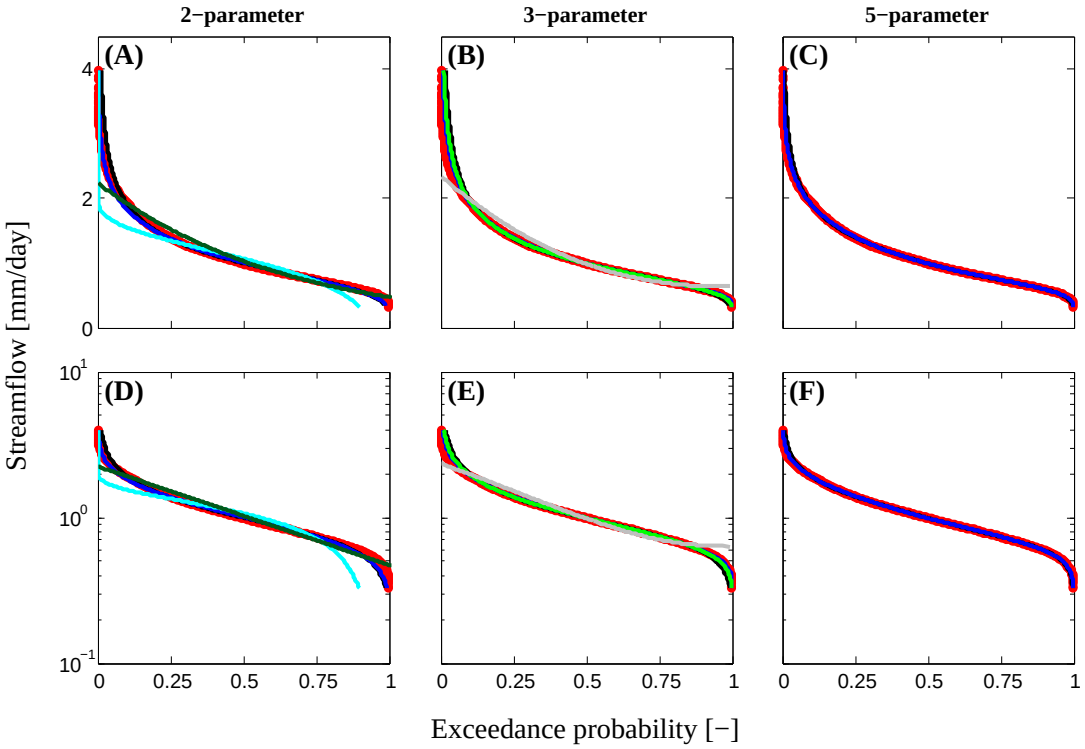

Figure 6. Comparison of the observed (red dots) and fitted (different lines) FDCs of the Kankakee river at Davis, IN, USA. The top (A-C) panel uses a linear scale of the streamflow values, whereas the bottom (D-F) panel uses a logarithmic scale. The different columns display the results of the 2 (left), 3 (middle) and 5 (right) parameter formulations.Color coding is used to differentiate between the FDC models of Table 1: VG (black), Kosugi (blue), Gumbel (cyan), Quimpo (dark green), GEV (light green) and Franchini and Suppo (gray).

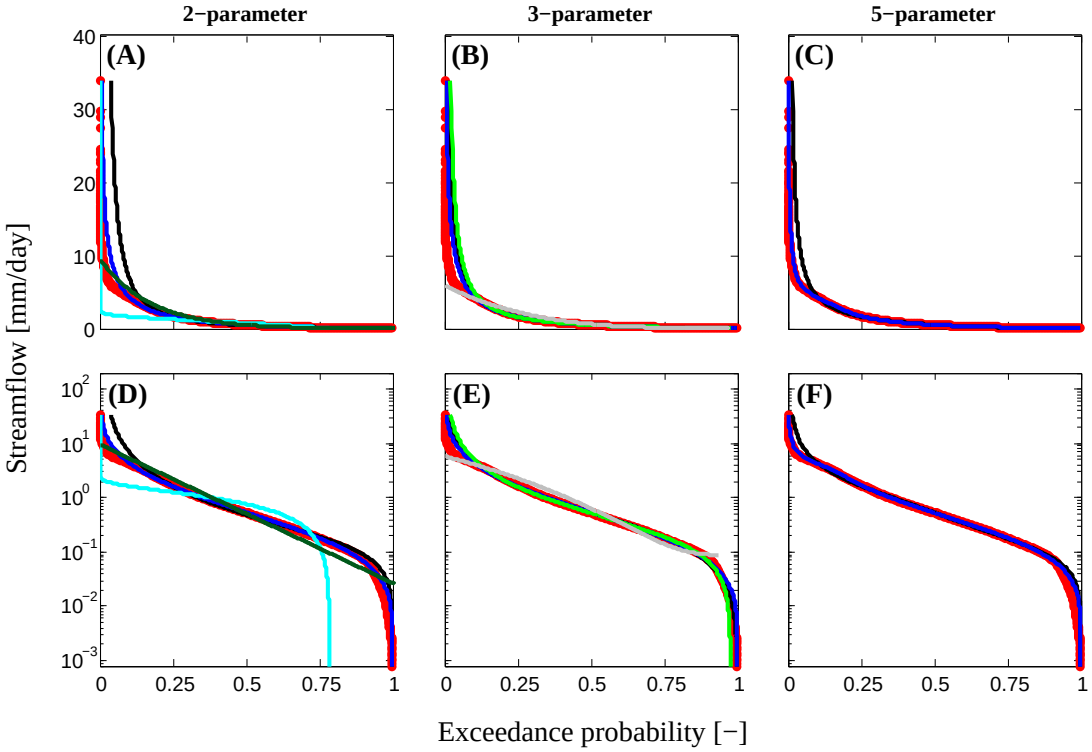

Figure 7. Comparison of the observed (red dots) and fitted (different lines) FDCs of the Little river near Horatio, AR, USA. A linear scale of the streamflow values is used in the top panel, whereas the bottom panel uses a logarithmic y-scale. The different columns display the results of the 2 (left), 3 (middle) and 5 (right) parameter formulations. The VG model is portrayed in black, and the Kosugi model in blue. The other FDC models proposed in the literature are displayed in cyan (Gumbel), dark green (Quimpo), light green (GEV) and gray (Franchini and Suppo).

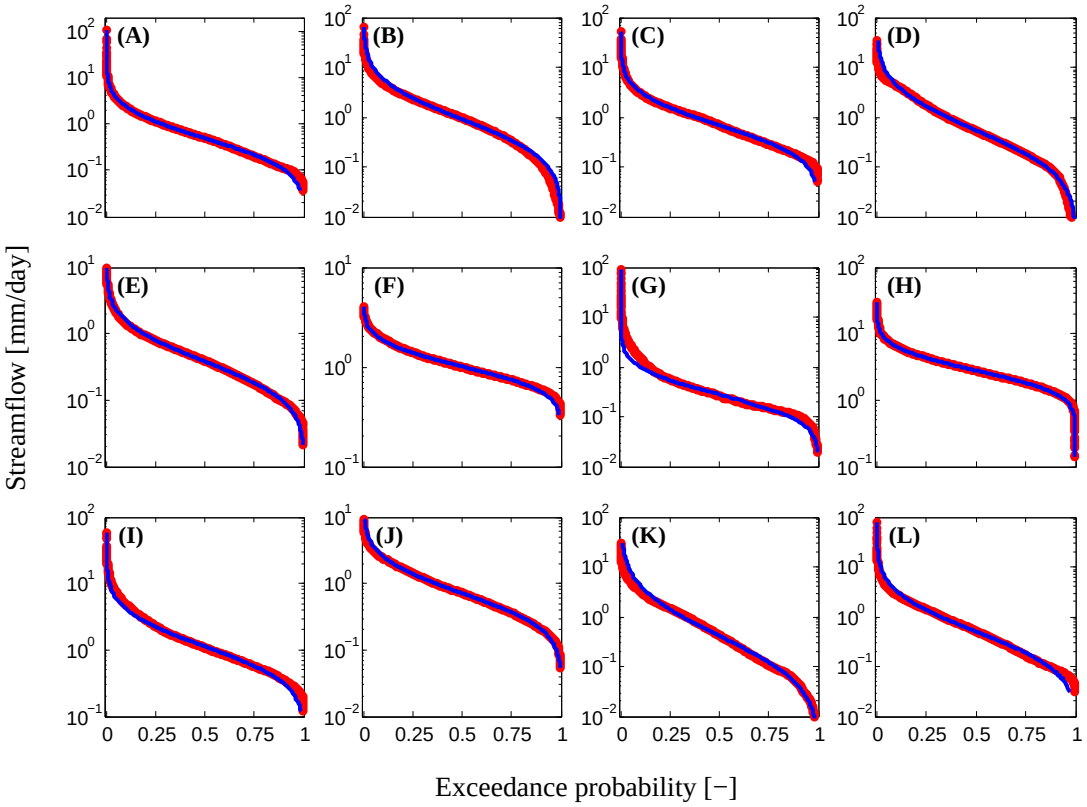

Figure 8. Comparison of the simulated FDCs of the 2-parameter Kosugi model (blue lines) against their observed counterparts (red dots) of the MOPEX data set. The different graphs correspond to the (A) SB Potomac, (B) Tygart Valley, (C) NF Holston, (D) Little, (E) Green, (F) Kankakee, (G) EF San Gabriel, (H) White, (I) Pemigewasset, (J) Little Pee Dee, (K) Licking, and (L) Genesee river basins, respectively, which are found in the states of West Virginia (A,B), Virginia, Arkansas, Illinois, Indiana, California, Washington, New Hampshire, South Carolina, Kentucky, and New York.

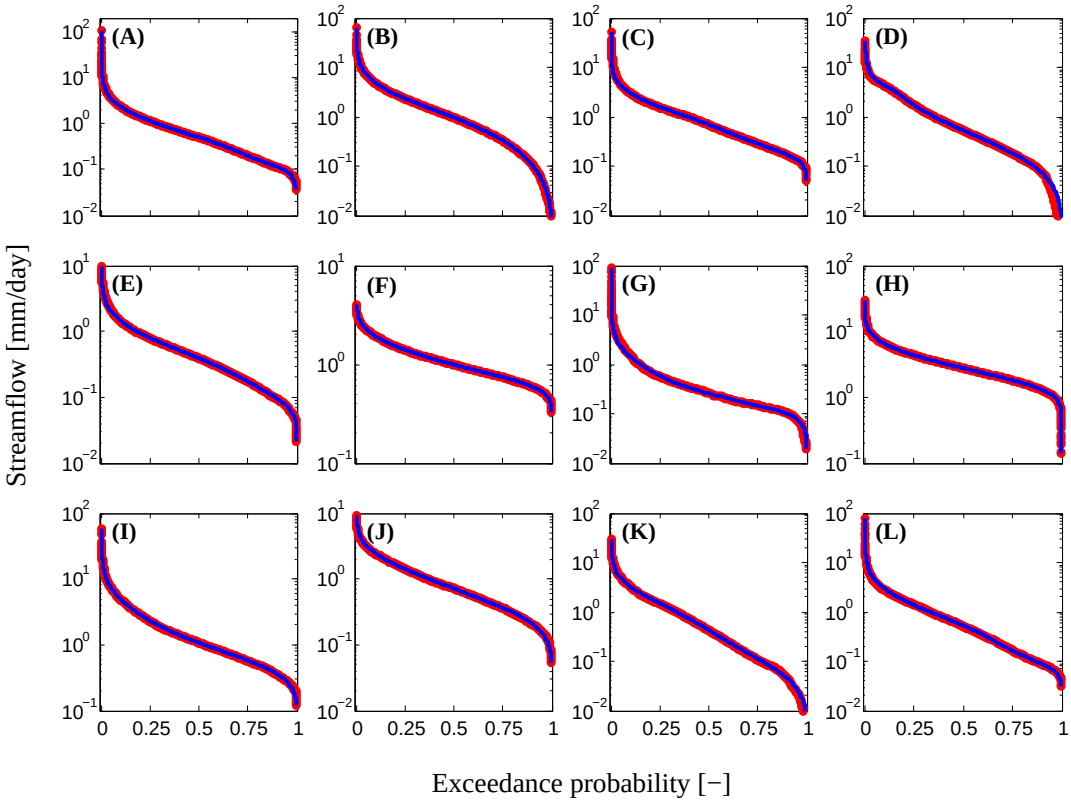

Figure 9. Comparison of the simulated FDCs of the 5-parameter Kosugi model (blue lines) against their empirical counterparts (red dots) of the MOPEX data set. The different graphs pertain to the (A) SB Potomac, (B) Tygart Valley, (C) NF Holston, (D) Little, (E) Green, (F) Kankakee, (G) EF San Gabriel, (H) White, (I) Pemigewasset, (J) Little Pee Dee, (K) Licking, and (L) Genesee river basins respectively which are located in the states of West Virginia (A,B), Virginia, Arkansas, Illinois, Indiana, California, Washington, New Hampshire, South Carolina, Kentucky, and New York.

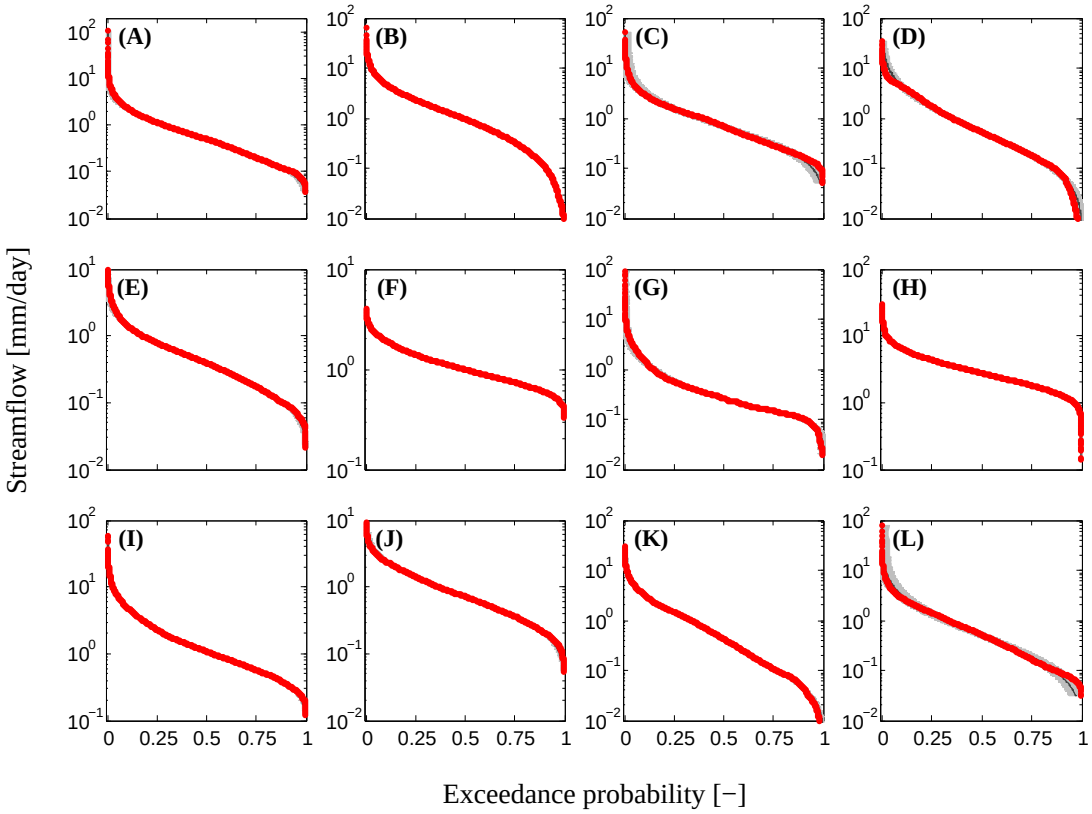

Figure 10. 95% simulation uncertainty ranges of the 5-parameter Kosugi model for the twelve different watersheds of Figure 8. The observed data are indicated with the red dots, whereas the 95% parameter and total uncertainty are displayed using the dark and light gray regions, respectively. The fit to the empirical FDCs is excellent and the parameter and model uncertainty therefore negligibly small.